Control of the Three Phase four-wire four-leg SAPF Using 3D-SVM Based on the Two Methods of Reference Signals Generating CV and SRF in the dqo-axes

[1]A. Chebabhi, [1]M. K. Fellah, [2] M. F. Benkhoris
[1]ICEPS Laboratory (Intelligent Control & Electrical Power Systems). Djillali Liabes University of Sidi Bel-Abbes. Algeria,
Alich7@gmail.com
chebabhiali@gmail.com
mkfelah@yahoo.fr
[2]IREENA Laboratory (Institut de Recherche en Electronique et Electrotechnique de Nantes Atlantique), University of Nantes at Saint Nazaire. France.
Mohammed-Fouad.Benkhoris@univ-nantes.fr

Abstract*: In this paper, the performance of the two algorithms of generating reference signals for three phase four-wire four-leg SAPF are compared in load conditions balance and unbalance. The algorithms that are used for this study are the synchronous reference frame theory (SRF) and cross-vector theory (CV), in the dqo-axes, and the voltage and current regulation is performed by the PI type controller, using the 3D-SVM technique to generate the switching signals, It is shown by simulation studies of the source current harmonics, the switching loss of the converter is reduced to the reference method with synchronous using 3D-SVM technical, Simulation results show the superiority of synchronous reference frame theory both in definition and compensation.*

Keywords: *Three phase four-wire four-legs SAPF, 3D-SVM, Zero sequence, PI, CV, SRF, dqo-axes.*

1. introduction

Le Distribution networks are faced with new challenges and new opportunities of an electrical system in full technological developments. From the technical viewpoint, the main change concerns the nature of network connected loads; firstly, conventional passive load have undergone a very important development, and secondly, new active loads have been connected to the network [1]. These new charges generate major disturbances in the power network such as voltage disturbances caused by the passage of perturbation currents as harmonic currents, reactive and unbalanced.

The technical of reducing harmonic currents, by passive LC filters [5], [7], [10], is generally formed by capacitors and inductors connected to the network. Each harmonic (5th, 7th, 11th, 13th) requires its own passive filter. This means that the filter can not be designed in general case, but must be designed according to each application. This solution has the advantages of simplicity and low cost. However, among the disadvantages are: designed for a specific application, the size and positioning of the filter elements, the risk of resonance problems.

The active power filters are a new solution for the compensation of harmonic pollution in power systems. We can distinguish two types of active filters, series and shunt. The shunt active power filter makes the compensation of harmonic currents and reactive power [2].The analysis of the operation of a three-leg active filter connected to a four-wire network shows that it cannot compensate for perturbations due to single-phase non-linear loads connected to a four-wire network. Harmonic currents circulating in the network remain partly compensated and amplitude of the zero sequence current is not reduced, to remedy it will be necessary to provide a four-leg shunt active filter [3]-[14].

Among the various topologies the three phase four-wire four-leg SAPF based on voltage source inverter is the most common one because of its good efficiency. Its performance depends on the adoptive control approaches. There are four major parts of an active power filter controller. The first is the reference signal generation technique, the second is that switching signals

generation techniques, the third is the controller of the system, and the fourth is the inverter to inject the compensating current into AC mains [4]-[19].

This paper presents the cross-vector theory and the synchronous reference frame theory in the *dqo-axes* for the generation of reference signals harmonic of a three phase four-wire four-leg SAPF, we will use the 3D-SVM technique for generating switching signals. The control reference currents and the capacitor voltage used in both are extracted from the proportional-integral regulator (PI).

The simulation results of the two methods discussed will be presented in order to prove the efficiency of these methods.

In Section II, we recall the main circuit principle of a three phase four-wire four-leg SAPF. In Section III, we present two algorithms of generating reference signals and zero sequence currents methods. In Section IV, we present the switching signals generation technique. In Section V we analyze the simulation results of the control system, and we finish with a conclusion where we the value of this control strategy.

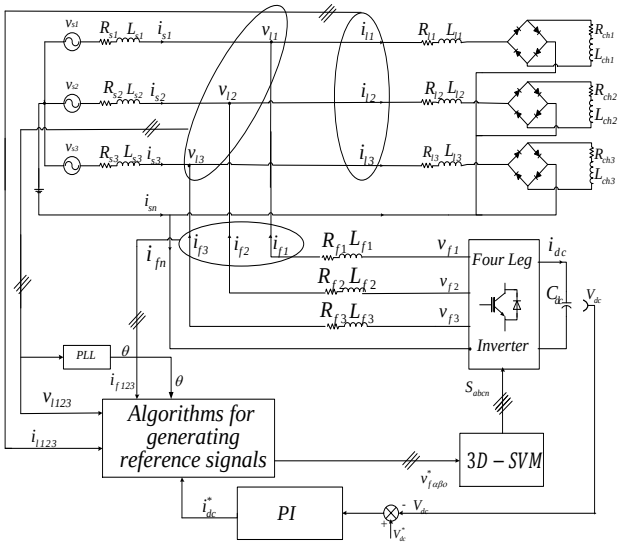

Fig. 1. Schematic block diagram of three phase four-wire four-legs shunt active power filter with 3D-SVM control technique

The filtering process is a three phase four-wire four-leg SAPF, that is can be partitioned to four essential elements are namely; signal conditioning, reference current generation, signal generation and four-leg inverter with a DC side capacitor as energy storage element [7]-[8]-[9]

2. System Modeling

The differential equations describing the dynamic model of the inverter are defined in *dqo-axes*, as given in equation (1):

$$\begin{cases} \dfrac{di_{fd}}{dt} = -\dfrac{R_f}{L_f} i_{fd} + \omega i_{fq} + \dfrac{1}{L_f} v_{fd} - \dfrac{1}{L_f} v_{ld} \\ \dfrac{di_{fq}}{dt} = -\dfrac{R_f}{L_f} i_{fq} - \omega i_{fd} + \dfrac{1}{L_f} v_{fq} - \dfrac{1}{L_f} v_{lq} \\ \dfrac{di_{fo}}{dt} = -\dfrac{R_f}{L_f} i_{fo} + \dfrac{1}{L_f} v_{fo} - \dfrac{1}{L_f} v_{lo} \\ \dfrac{dV_{dc}}{dt} = -\dfrac{1}{C} i_{dc}^{*} = \dfrac{P_{dc}^{*}}{CV_{dc}} \end{cases} \quad (1)$$

3. Algorithms of generating reference signals

3.1 The cross-vector theory

Cross-vector theory defines instantaneous active and reactive power respectively by the scalar and vector product of the voltage and the current space vectors in the time domain in a three-phase four-wire system [7], [15]**.** Here, the instantaneous active and reactive powers have the same physical meaning of the instantaneous real and imaginary powers in pq theory. The authors prefer to express it as instantaneous real and imaginary power to distinguish it from the traditional definition of active and reactive power in the frequency domain.

Fig. 2 present schematic principal of the cross-vector method [16]. The instantaneous power is calculated as follows:

$$\begin{bmatrix} p_l \\ q_l \\ p_{l\alpha} \\ q_{l\beta} \end{bmatrix} = \begin{bmatrix} v_{lo} & v_{l\alpha} & v_{l\beta} \\ 0 & -v_{l\beta} & v_{l\alpha} \\ v_{l\beta} & 0 & -v_{lo} \\ -v_{l\alpha} & v_{lo} & 0 \end{bmatrix} \begin{bmatrix} i_{l\alpha} \\ i_{l\beta} \\ i_{lo} \end{bmatrix} \quad (2)$$

From equation (2), we can deduce the corresponding current components:

$$\begin{bmatrix} i_{l\alpha} \\ i_{l\beta} \\ i_{lo} \end{bmatrix} = \begin{bmatrix} v_{lo} & v_{l\alpha} & v_{l\beta} \\ 0 & -v_{l\beta} & v_{l\alpha} \\ v_{l\beta} & 0 & -v_{lo} \\ -v_{l\alpha} & v_{lo} & 0 \end{bmatrix}^{-1} \begin{bmatrix} p_l \\ q_{lo} \\ p_{l\alpha} \\ q_{l\beta} \end{bmatrix} \quad (3)$$

$$\begin{bmatrix} i_{lo} \\ i_{l\alpha} \\ i_{l\beta} \end{bmatrix} = A' \begin{bmatrix} v_{lo} & 0 & v_{l\beta} & v_{l\alpha} \\ v_{l\alpha} & -v_{l\beta} & 0 & v_{lo} \\ v_{l\beta} & v_{l\alpha} & -v_{lo} & 0 \end{bmatrix} \begin{bmatrix} p_l \\ q_{lo} \\ q_{l\alpha} \\ q_{l\beta} \end{bmatrix} \quad (4)$$

With: $A' = \dfrac{1}{v_{l\alpha}^2 + v_{l\beta}^2 + v_{lo}^2}$

Equation (4) so becomes:

$$\begin{bmatrix} i_{fo}^* \\ i_{f\alpha}^* \\ i_{f\beta}^* \end{bmatrix} = A' \begin{bmatrix} v_{lo} & 0 & v_{l\beta} & v_{l\alpha} \\ v_{l\alpha} & -v_{l\beta} & 0 & v_{lo} \\ v_{l\beta} & v_{l\alpha} & -v_{lo} & 0 \end{bmatrix} \begin{bmatrix} p_f^* \\ q_{fo}^* \\ q_{f\alpha}^* \\ q_{f\beta}^* \end{bmatrix} \quad (5)$$

The inverse Concordia transform calculates the reference currents in the *abc-axes* as follows:

$$\begin{bmatrix} i_{f1}^* \\ i_{f2}^* \\ i_{f3}^* \end{bmatrix} = \sqrt{\frac{2}{3}} \begin{bmatrix} 1 & 0 & \frac{1}{\sqrt{2}} \\ -\frac{1}{2} & \frac{\sqrt{3}}{2} & \frac{1}{\sqrt{2}} \\ -\frac{1}{2} & -\frac{\sqrt{3}}{2} & \frac{1}{\sqrt{2}} \end{bmatrix} \begin{bmatrix} i_{f\alpha}^* \\ i_{f\beta}^* \\ i_{fo}^* \end{bmatrix} \quad (6)$$

The Fig.2 shows the diagram of the cross vector method.

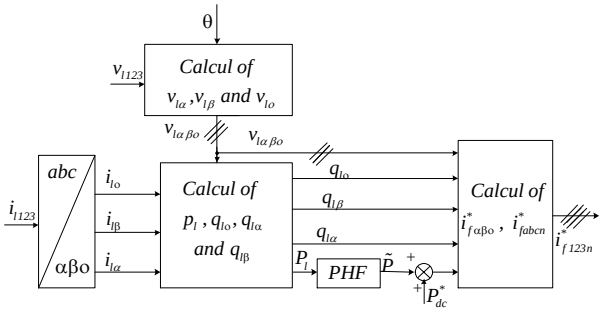

Fig. 2 Schematic diagram of the cross-vector theory

3.2 Synchronous Reference Frame Theory (SRF)

The SRF theory gave very good results for the compensation of three phase three wire electricity network. For three phase four wire electricity networks, a theory based on the modification of the cross-vector theory of *dqo-axes*, has been proposed [20].

Fig. 4 shows the basic principle of this SRF theory applied to a three phase four wire four-leg SAPF [21].

The SRF theory firstly requires the transformation of the three-phase load currents in the *αβo-axes* as follows:

$$\begin{bmatrix} i_{l\alpha} \\ i_{l\beta} \\ i_{lo} \end{bmatrix} = \sqrt{\frac{2}{3}} \begin{bmatrix} 1 & -\frac{1}{2} & -\frac{1}{2} \\ 0 & \frac{\sqrt{3}}{2} & -\frac{\sqrt{3}}{2} \\ \frac{1}{\sqrt{2}} & \frac{1}{\sqrt{2}} & \frac{1}{\sqrt{2}} \end{bmatrix} \begin{bmatrix} i_{l1} \\ i_{l2} \\ i_{l3} \end{bmatrix} \quad (7)$$

We obtain in *dqo-axes* the following currents:

$$\begin{bmatrix} i_{ld} \\ i_{lqo} \\ i_{lq\alpha} \\ q_{lq\beta} \end{bmatrix} = \begin{bmatrix} 0 & \sin(\theta) & -\cos(\theta) \\ 0 & \cos(\theta) & \sin(\theta) \\ -\cos(\theta) & 0 & 0 \\ -\sin(\theta) & 0 & 0 \end{bmatrix}^{-1} \begin{bmatrix} i_{lo} \\ i_{l\alpha} \\ i_{l\beta} \end{bmatrix} \quad (8)$$

The signals $\sin(\theta)$ and $\cos(\theta)$ related to the mains voltage,

The currents i_{chd} and i_{chq} can be expressed as the sum of two components, a continuous and another alternative, such as:

$$\begin{bmatrix} i_{ld} \\ i_{lq} \end{bmatrix} = \begin{bmatrix} \bar{i}_{ld} & \tilde{i}_{ld} \\ \bar{i}_{lq} & \tilde{i}_{lq} \end{bmatrix} \quad (9)$$

With $\bar{i}_{chd}$, $\bar{i}_{chq}$ are the direct components of i_{chd} and i_{chq}, and $\tilde{i}_{chd}$, $\tilde{i}_{chq}$ alternative components of i_{chd} and i_{chq} respectively.

The filter reference currents are expressed in *dqo-axes* by:

$$\begin{bmatrix} i_{lo}^* \\ i_{l\alpha}^* \\ i_{l\beta}^* \end{bmatrix} = \begin{bmatrix} 0 & 0 & -\cos(\hat{\theta}) & -\sin(\hat{\theta}) \\ \sin(\hat{\theta}) & \cos(\hat{\theta}) & 0 & 0 \\ -\cos(\hat{\theta}) & \sin(\hat{\theta}) & 0 & 0 \end{bmatrix} \begin{bmatrix} i_{fd}^* \\ i_{fq}^* \\ i_{fq\alpha}^* \\ i_{fq\beta}^* \end{bmatrix} \quad (10)$$

With: $\begin{bmatrix} i_{fd}^* \\ i_{fq}^* \\ i_{fq\alpha}^* \\ i_{fq\beta}^* \end{bmatrix} = \begin{bmatrix} i_{ld} \\ i_{lq} \\ i_{lq\alpha} \\ i_{lq\beta} \end{bmatrix}$.

The inverse Concordia transform calculates the reference currents in the *abc-axes* as follows:

$$\begin{bmatrix} i_{f1}^* \\ i_{f2}^* \\ i_{f3}^* \end{bmatrix} = \sqrt{\frac{2}{3}} \begin{bmatrix} 1 & 0 & \frac{1}{\sqrt{2}} \\ -\frac{1}{2} & \frac{\sqrt{3}}{2} & \frac{1}{\sqrt{2}} \\ -\frac{1}{2} & -\frac{\sqrt{3}}{2} & \frac{1}{\sqrt{2}} \end{bmatrix} \begin{bmatrix} i_{f\alpha}^* \\ i_{f\beta}^* \\ i_{fo}^* \end{bmatrix} \quad (11)$$

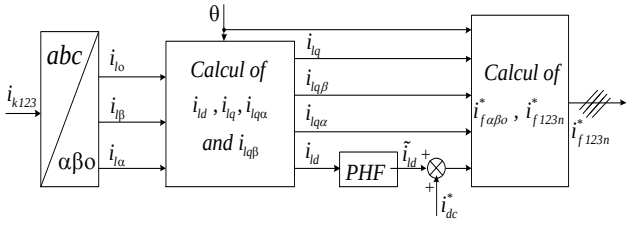

Fig. 3 Schematic diagram of the Synchronous Reference Frame theory

4. Technique for generating switching signals

The objective of control is to generate the opening and closing commands of the switches, so that current is injected by the inverter currents nearest reference.

4.1 Three Dimensional Space Vector Modulation with Null Vector

The major advantage of a four-leg inverter is that the DC bus utilization can be improved by using 3D Space

Vector Modulation [8]-[9].

4.2 Prism identification

Six prisms in the 3D space can be identified and numbered as Prisms I through VI (Fig. 3). Within the selected prism, there are six non-zero switching state vectors and two zero switching state vectors. Fig. 4 shows the physical positions of the switching state vectors in *αβo-axes* [10]-[13].

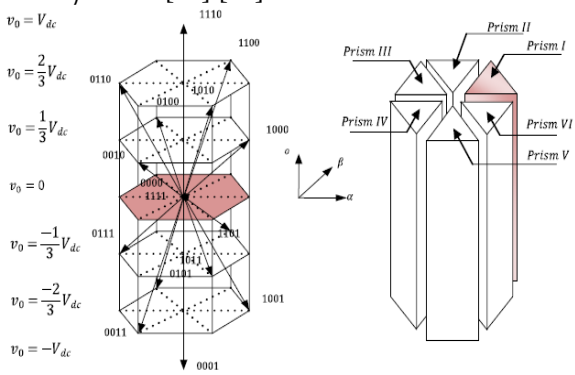

Fig. 4 Voltage vectors in abc system in the *αβo-axes*, and the selection of prism.

4.3 Tetrahedron identification

The tetrahedron is formed by three non-zero voltage vectors and two other zero vectors, as shown in Fig. 5. Fig. 6 describes the representation of tetrahedron 1 plans belonging to prism I [10]-[11].

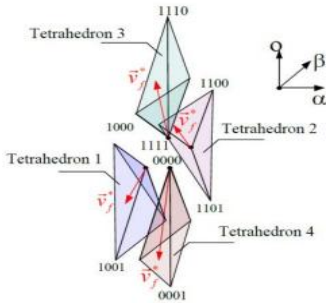

Fig. 5 Representation of tetrahedra in the prism I

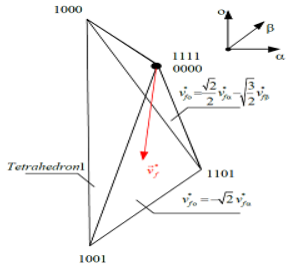

Fig. 6 Projection of the reference vector on the adjacent vectors

4.4 Duty Cycle Calculation

For the tetrahedron i of the prism j, the states vectors of the inverter (v_x, v_y, v_z, v_1, v_{16}) are the adjacent vectors to the reference voltage vector. These vectors are applied individually for certain periods tx, ty, tz and t0, such that the vector $\overline{v}^*$ is equal to the mean value of those vectors for a period of switching: [12]

$$\overline{v}^* = \overline{V}_x + \overline{V}_y + \overline{V}_z + \overline{V}_0 \tag{12}$$

With: $x, y, z \in \{2,.....,15\}$ *and* $o \in [1,16]$.

The mean reference vector is expressed by:

$$\overline{v}^* = \frac{1}{T_h}\int_t^{t+T_h} \vec{v}^*\, dt \tag{13}$$

As the period of switching is very small, the mean voltage value can be considered as constant; and as the vectors V_x, V_y, V_z *et* V_0 are fixed, it follows that:

$$\overline{V}_i = \frac{1}{T_h}\int_t^{t+t_{ii}} V_i dt = \frac{1}{T_h} V_i t_i \tag{14}$$

With i=x,y,z,0.

Then

$$T_h v^* = t_x V_x + t_y V_y + t_z V_z + t_0 V_0 \tag{15}$$

$$t_0 = T_h - t_x - t_y - t_z \tag{16}$$

4.5 The Control Pulses Generation

The fig. 7 shows, on a switching period, the distribution of voltage vectors to be applied in the first prism tetrahedron [9].

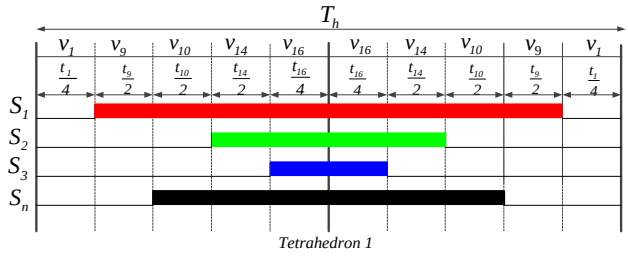

Fig. 7 Principle of generation in the pulses by 3D-SVM

5. Simulation results and discussion

The simulations were performed considering a three-phase four-wire four-leg SAPF feeding three unbalanced nonlinear loads, as shown in fig. 1. The parameters of SAPF are shown in Table 1.

The simulation of the three phases four-wire four-leg SAPF was carried out under the following conditions:

- The switching frequency: f_s= 14 kHz.
- The reference voltage: $V_{dc\ ref}$ = 800 V.

Table 1: System parameters for simulation and load specifications

Capacitance of the capacitor	5 mF
Coupling impedance R_f, L_f	0.1 mΩ, 0.1 mH
The source voltage and frequenc	220 V, 50Hz
Source impedance R_s, L_s	1 mΩ, 1 mH
Line impedance R_{ch}, L_{ch}	1 mΩ, 1 mH
Load impedance R_l, L_l	5Ω, 10 mH

5.1 Simulation du système avant le filtrage

The simulation results of the system before compensation are given in fig. 8.

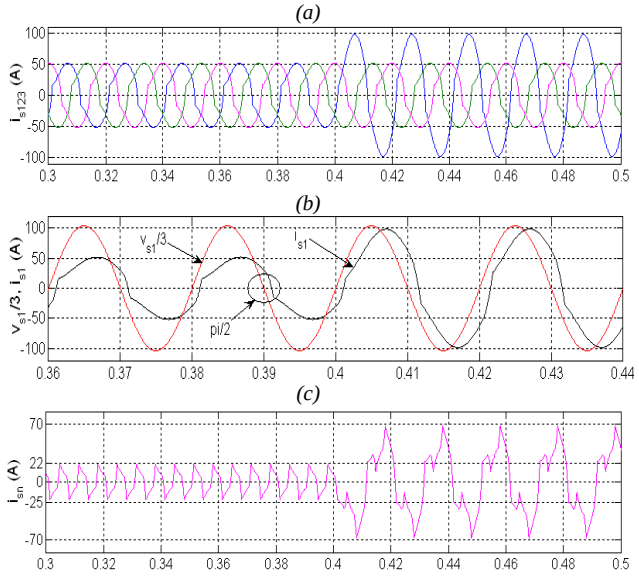

Fig. 8 Simulation results before compensation (a) Phase Currents, (b) Voltage and current source of the first phase, (c) Neutral Current

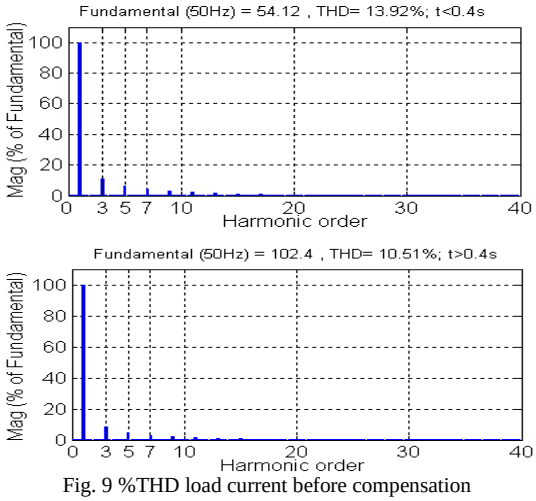

Fig. 9 %THD load current before compensation

The fig. (8-a) shows the current waveform of the load, it is a highly non-sinusoidal current and deformed and there is not in sync with the corresponding voltages (power factor is Fp = 0). The fig. (8-c) shows the shape of neutral current with a maximum value of 22A in the balanced case and 70A in the unbalanced case. Fig. (9-a,b) shows the first phase source current's THD. Before unbalanced load (t<0.4s), the total harmonic distortion (THD) is 13.92%, when after (t >0.4s) it's 10.51%.

5.2 Simulation with The cross-vector theory

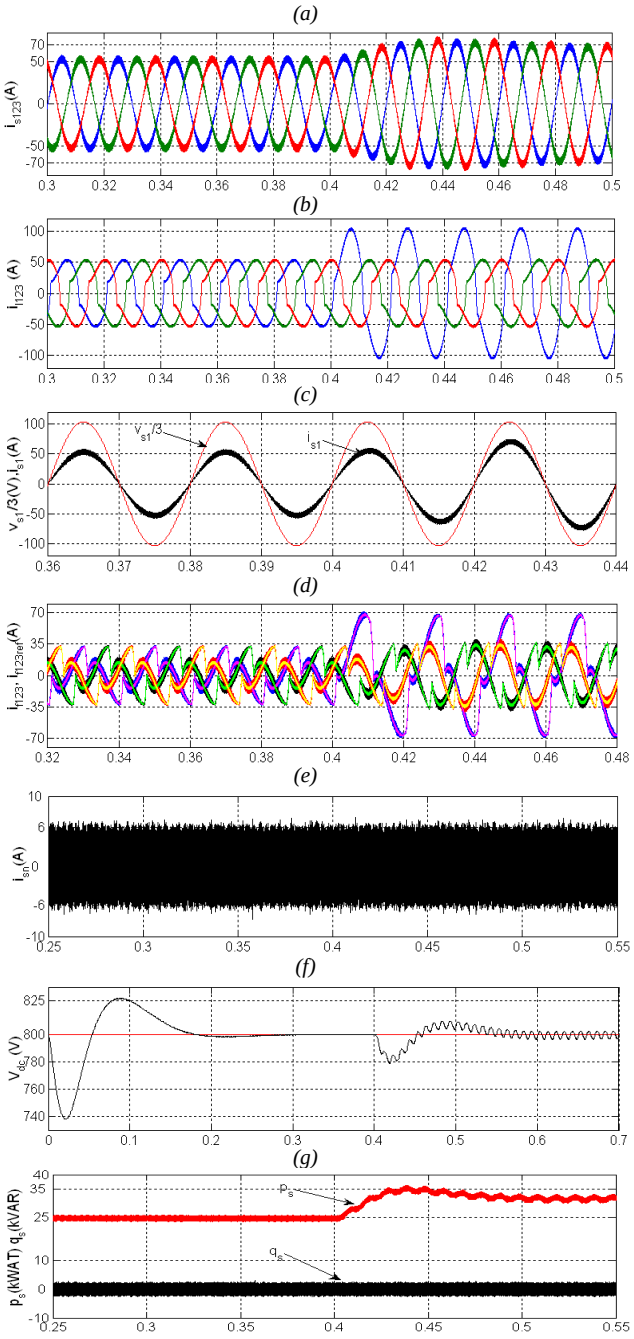

Fig.10 The cross-vector theory simulation results: (a) source currents after compensation (b) load current after compensation (c) Voltage and current source of the first phase after filtering (d) Injected currents by

the active filter (e) Neutral current after filtering,(f) DC link voltage, (g) Real and imaginary powers.

5.3 Simulation with The SRF theory

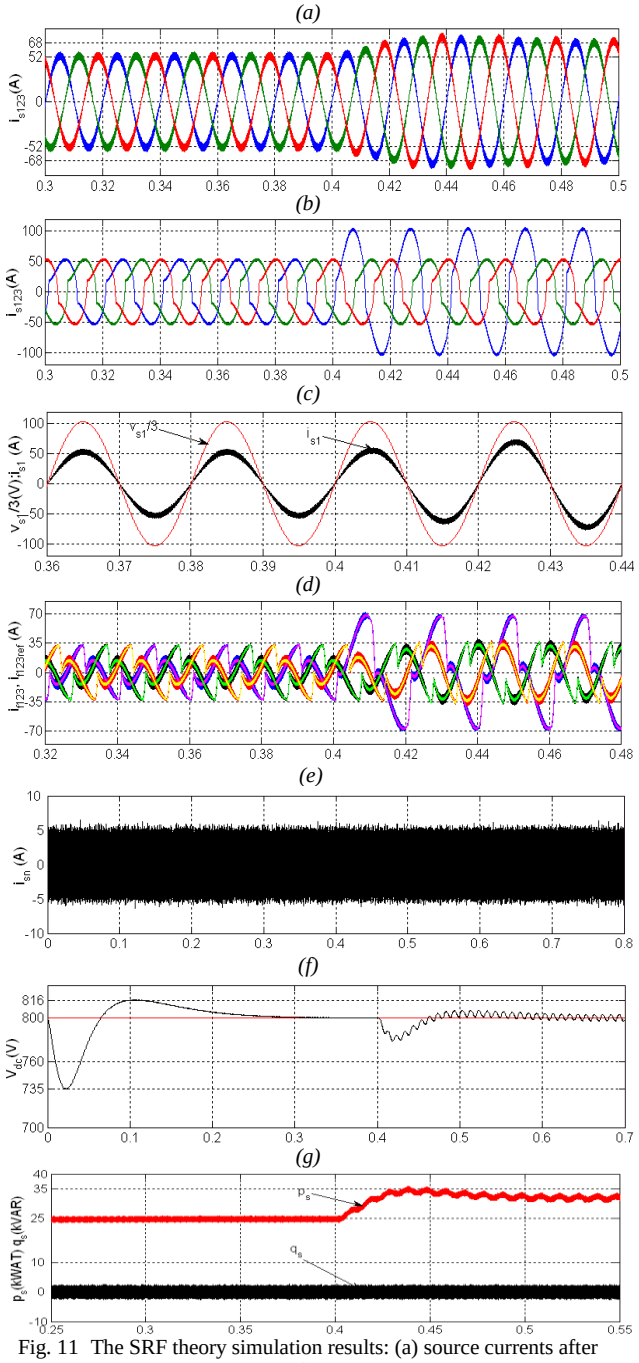

Fig. 11 The SRF theory simulation results: (a) source currents after compensation (b) load current after compensation (c) Voltage and current source of the first phase after filtering (d) Injected currents by the active filter (e) Neutral current after filtering,(f) DC link voltage, (g) Real and imaginary powers.

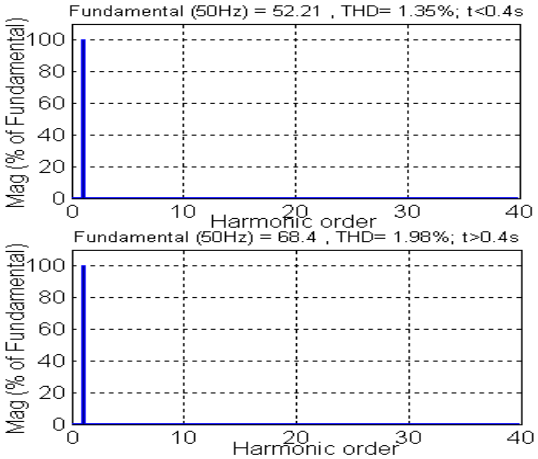

Fig. 12 %THD source current before and after unbalanced load with the cross-vector theory

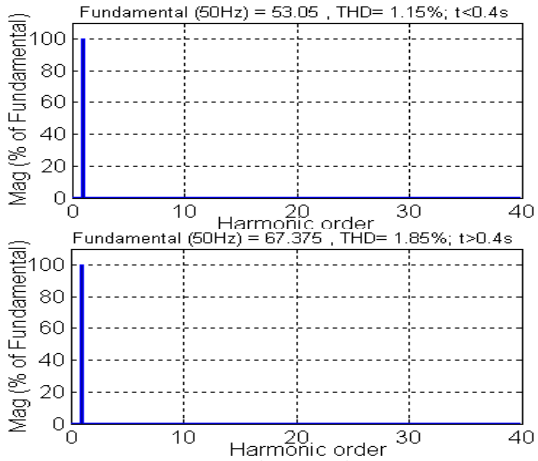

Fig. 13 %THD source current before and after unbalanced load with the SRF theory

The figs. (10.11-a) shows the source current waveform after filtering is sinusoidal. The figs. (10.11 – b) represent the load current form, it is non-sinusoidal current and highly deformed. It is noted that the current network is still in phase with the corresponding voltage, and the power factor is unitary as shown in figs. (10.11-c). The figs. (10.11-d) represents the active filter injected currents. The figs. (10.11-e) show that after compensation the neutral current is in the range of ±6 A with CV theory and the range of ±5 A with SRF theory. The capacitor voltage is stabilized at its reference value with a small static error as shown in figs (10.11-f). Figs (10.11-g) show the real and imaginary power of source.It can be seen here that the active power p_s is delivered almost constantly by the source although the loads demand a fluctuated active power.

Observing the reactive power q_s waveform, the source is successfully forced not to supply the reactive power as the value of q is always around 0. Figs. (12-13) show the first phase source current's THD for the two theories.

Before unbalanced load (t<0.4s), the total harmonic distortion (THD) is 1.35% for the CV theory and 1.15% for the SRF theory, when after (t >0.4s) it's 1.98% for the CV theory and 1.85% for the SRF theory.

6. Conclusion

For industrial equipment and consumer products, improving the quality of energy is a prerequisite. The SAPF offers better performance than other methods of compensation. the structure of the three phase four-wire four-leg Shunt Active Power Filter allowing compensation of harmonic currents in the network, reducing the amplitude of the zero sequence current and improve the power factor.

The results from the simulation of two algorithms of control, we showed that these two algorithms can compensate for harmonic currents in the network and reducing the magnitude of the zero sequence current, The two algorithms, performed into *dqo-axes*, was implemented using 3D SVM. However, we demonstrate that the algorithm (SRF) is better because it reduces the rate THD network side.

The table 2 gives the THD and amplitude of the neutral current comparison of 3D-SVM control technique with CV and SRF control strategy using Matlab/Simulink.

Table 2: Comparison of the different techniques

	CV		SRF	
	Balanced Load	Unbalanced Load	Balanced Load	Unbalanced Load
Source current THD %	1.35%	1.98%	1.15%	1.85%
The amplitude of the neutral current (A)	6 A		5 A	

7. References

[1] Akagi. H, Kanazawa Y, Nabae A. "Instantaneous reactive power compensators comprising switching devices without energy storage components". IEEE Transactions on Industry Applications, 2008, vol:20, Issue: 3, pp: 625–630.

[2] H. Akagi, "The State Of The Art of Active Filters for Power Conditioning", IEEE, European Conference on Power Electronics and Applications, 2005.

[3] M. Ucar, E. Ozdemir, "Control of a 3-Phase 4-leg active power filter under non ideal mains voltage condition", Electric Power Systems Research, vol : 78, Issue : 1, 2008, pp :58–73.

[4] N. V. wanath, A. K. Kapok "Performance Estimation of HCC and SVPWM Current Control Techniques on Shunt Active Power Filters" IEEE, International Conference on Power, Control and Embedded Systems (ICPCES), Nov-29: Dec-1, 2010, pp: 1 – 6.

[5] S. Pataki, A. K. Panda "Real-time performance analysis and comparison of various control schemes for particle swarm optimization-based shunt active power filters" Electrical Power and Energy Systems,vol:52, 2013, pp:185–197.

[6] B. Exposto, H. Conclaves, J. G. Pinto, J. L. Alonso, C. Couto, "Three Phase Four Wire Shunt Active Power Filter from Theory to Industrial Facility Tests," IEEE, 11th International Conference on Electrical Power Quality and Utilisation (EPQU) 17-19 Oct, 2011, pp: 1 – 5.

[7] C.-S. Lam, X.-X. Cui, W. H. Choi, M. C. Wong, Y.-D. Han. "Minimum DC-Link Voltage Design of Three-Phase Four-Wire Active Power Filters", IEEE, 13th Workshop on Control and Modeling for Power Electronics (COMPEL), 10-13 June, 2012, pp: 1-5.

[8] A. Chichi, A. Gaeta, A. Benoudjit, "Four legged Active Power Filter Compensation For A Utility Distribution System", Journal of Electrical Engineering, vol. 55, 2004.

[9] D. Mingxuan, H. Zhihao, W. Jian, X. Dianguo, H. Key " Study on Three-Leg-Based Three-Phase Four-Wire Shunt Active Power Filter" IEEE 7th International Conference on Power Electronics and Motion Control - ECCE , Asia, June 2-5, 2012, pp: 552 - 556.

[10] B. K. Bose, "Modern Power Electronics and AC Drives"

[11] H. Golwala, R. Chudamani, "Comparative Study of Switching Signal Generation Techniques for Three Phase Four Wire Shunt Active Power Filter", IEEE International Electric Machines & Drives Conference (IEMDC) , 15-18 May, 2011, pp: 1409 – 1414.

[12] H. Golwala, R. Chudamani," Simulation of three-phase four-wire shunt active power filter using novel switching technique ", International Conference on Power Electronics, Drives and Energy Systems (PEDES), 2010.

[13] H. Golwala, R. Chudamani « Comparative Study of Switching Signal Generation Techniques for Three Phase Four Wire Shunt Active Power Filter" 2011 IEEE International Electric Machines & Drives Conference (IEMDC).

[14] A. Chaghi, Augusta, A.Benoudjit, "Four legged Active Power Filter Compensation For a Utility Distribution System", Journal of Electrical Engineering, vol: 55, NO: 1-2, 2004.

[15] H. Kim, F. Blaabjerg, B. Bak-Jensen, J.Choi "Instantaneous power compensation in three-phase systems by using p-q-r theory", IEEE 32nd Annual Specialists Conference Power Electronics vol:17 , Issue: 5, 2001.

[16] F.Z. Peng, G.W.Jr. Ott, D.J.Adams''Harmonic and reactive power compensation based on the generalized instantaneous reactive theory for three-phase four wire systems", IEEE Trans, on Power Electronic, Vol: 13, N: 6, pp. 1174-1181, 1998.

[17] P. Kanjiya, V. Khadkikar,Hatem H. Zeineldin"A Non-Iterative Optimized Algorithm for Shunt Active Power Filter under Distorted and Unbalanced Supply Voltages" IEEE Trans, on Industrial Electronics, vol:60, No:12, 2013, pp: 5376 - 5390.

[18] A. S. Abu Hasim, M. H. N. Talib, Z. Ibrahim « Comparative Study of Different PWM Control Scheme for Three-Phase Three - Wire Shunt Active Power Filter » IEEE, International Conference on Power Engineering and Optimization (PEDCO) Melaka, Malaysia, 6-7 June, 2012, pp: 119-123.

[19] E. J. Acordi, L.B.G. Campanhol, S. A. O. Silva, C. B. Nascimento and A. Goedtel "A Study of Shunt Active Power Filters Applied to Three-Phase Four-Wire Systems" International Conference on Renewable Energies and Power Quality (ICREPQ'12) Santiago de Compostela (Spain), 28th to 30th March, 2012.

[20] K. Bhattacharjee " Design and simulation of synchronous reference frame based shunt active power filter using simulink" National Conference on Challenges in Research and Technology in the Coming Decades (CRT 2013), 27-28 Sept 2013 , pp: 1-7.

[21] K. Bhattacharjee, "Harmonic mitigation by SRF theory based active power filter using adaptive hysteresis control " Conference Power and Energy Systems: Towards Sustainable Energy , 13-15 March, 2014 , pp: 1- 6.